Available online at www.sciencedirect.com

SciVerse ScienceDirect

Journal of the European Ceramic Society 32 (2012) 449–456

www.elsevier.com/locate/jeurceramsoc

Structural and electrical properties of 0.57PSN–0.43PT ceramics prepared by mechanochemical synthesis and sintered at low temperature

Hana Uršič [a,*], Jenny Tellier [a,b], Janez Holc [a], Silvo Drnovšek [a], Marija Kosec [a]

[a] *Electronic Ceramics Department, Jožef Stefan Institute, Jamova 39, SI-1000 Ljubljana, Slovenia*

[b] *Science des Procédés Céramiques et de Traitements de Surface, UMR 6638 CNRS, Centre Européen de la Céramique, 12 rue Atlantis, 87068 Limoges Cedex, France*

Received 18 April 2011; received in revised form 11 August 2011; accepted 18 August 2011
Available online 9 September 2011

Abstract

In this investigation we show that the dielectric, ferroelectric and piezoelectric properties of stoichiometric $0.57Pb(Sc_{1/2}Nb_{1/2})O_3$–$0.43PbTiO_3$ (0.57PSN–0.43PT) ceramics prepared by mechanochemical synthesis are comparable or even better than the properties of 0.57PSN–0.43PT ceramics with Nb doping, which was proposed to enhance the electrical properties. Here, the stoichiometric ceramic was sintered to 97% of theoretical density at a temperature of 1000 °C, which is 200–300 °C lower than previously reported. The dielectric constant ε, remnant polarization P_r, piezoelectric coefficient d_{33}, coupling coefficients k_p and k_t and mechanical quality factor Q_m of the ceramics prepared by mechanochemical synthesis were 2200, 43 μC/cm^2, 570 pC/N, 0.71, 0.56 and 38, respectively.

The effects of the poling field on the structural and electrical properties of the 0.57PSN–0.43PT ceramics were investigated. The results show that the ratio of the monoclinic to the tetragonal phases is influenced by the application of the poling electric field. The non-poled ceramics contain 71% of the monoclinic phase and 29% of the tetragonal phase. The highest d_{33}, k_p and k_t were measured for ceramics poled at an electric field of 3 kV/mm. For these poled ceramics a phase determination of 86% monoclinic phase and 14% tetragonal phase was obtained from Rietveld refinements.

Keywords: Mechanochemical synthesis; Sintering; Dielectric properties; Ferroelectric properties; Piezoelectric properties

1. Introduction

The relaxor-based $Pb(Mg_{1/3}Nb_{2/3})O_3$–$PbTiO_3$ (PMN–PT) and $Pb(Zn_{1/3}Nb_{2/3})O_3$–$PbTiO_3$ (PZN–PT) ceramics, with a composition near to the morphotropic phase boundary (MPB), exhibit a high dielectric constant and excellent piezoelectric properties, and are suitable for applications in actuators, sensors and capacitive devices.[1,2] However, their relatively low Curie temperature T_c (around 170 °C for PMN–PT and 180 °C for PZN–PT with its composition on the MPB) may greatly limit their usefulness in many fields, such as automotive and aerospace sensors, where a broad operating-temperature range is required. Therefore, new relaxor-PT systems with both high transition temperatures and good dielectric, ferroelectric and piezoelectric properties are desired.[3] The $Pb(Sc_{1/2}Nb_{1/2})O_3$–$PbTiO_3$ (PSN–PT) material meets these requirements and is therefore an attractive choice for applications at higher temperatures.[3–5]

The PSN–PT solid–solution system has not been well studied in comparison with the PMN–PT and PZN–PT systems, in fact only a few studies were carried out so far. The pioneering study of the phase diagram of the PSN–PT system was made by Tennery et al. in 1968.[6] Fifteen years later it was proposed that doping with niobium in these PSN–PT ceramics enhances the electrical properties.[7–10] The Nb-doping increases the electrical resistivity of PSN–PT material by two orders of magnitude, compared with non-doped samples, which promotes the poling of Nb-doped PSN–PT piezoelectric materials under a high electric field.[7,8] In the literature[11,12] it is also reported that Nb-doped $Pb(Zr,Ti)O_3$ (PZT) ceramics exhibit a low conductivity, a low coercive field, are more easy to pole and possess high piezoelectric coefficients in comparison with non-doped PZT. Donor dopants, such as Nb^{5+}, in place of (Zr,Ti), are compensated for either by electrons or doubly negatively charged lead vacancies V''_{Pb}.[11,12] Adding excess of niobium oxide to PSN–PT

* Corresponding author. Tel.: +386 1 477 3414; fax: +386 1 477 3887.
E-mail address: hana.ursic@ijs.si (H. Uršič).

0955-2219/$ – see front matter © 2011 Elsevier Ltd. All rights reserved.
doi:10.1016/j.jeurceramsoc.2011.08.033

material (in the literature[7–10] this is referred to as "Nb-doping" of PSN–PT material) could also introduce V''_{Pb} into the material. However, the mechanism of increased electrical resistivity of Nb-doped PSN–PT is still not well understood. Later, doping with iron in PSN–PT ceramics was also studied; however, the properties were not enhanced.[13] Also, recently the existence of a monoclinic phase with the space group Pm (subsequently called the monoclinic Pm phase in the text) between the rhombohedral phase with the space group R3m and the tetragonal phase with the space group P4mm (subsequently called the tetragonal P4mm phase) was reported in the phase diagram of the PSN–PT solid solution.[3,4] The most recent work reported on the growth and characterization of 0.58PSN–0.42PT single crystals.[14]

The functional properties of relaxors and relaxor-ferroelectrics are critically dependent on the chemical homogeneity of the materials, as shown in Refs.[15,16] The columbite method is commonly used to minimize the problem of the non-homogeneity of the material and in previous literature this method was already used for the preparation of PSN–PT.[5,7,9,10] In this work a mechanochemical synthesis method was used to obtain chemically homogeneous, fine particle PSN–PT powder. Mechanochemical synthesis is a powerful technique for synthesizing a variety of advanced materials. It has already been used for the preparation of several lead-based ceramics: PZT,[17] $Pb(Mg_{1/3}Nb_{2/3})O_3$,[18,19] PMN–PT,[20–22] and PZN–PT.[23] The aim of our work was to study the structural and electrical properties of 0.57PSN–0.43PT ceramics prepared from a mechanochemically activated powder and to compare them with the previously reported properties of PSN–PT ceramics with MPB compositions.

In the literature the PSN–PT ceramics with MPB compositions are usually poled with an electric field of 2.5–3 kV/mm at temperatures between 120 and 190 °C.[6–9,13,24] To the best of the authors' knowledge no systematic study of the influence of the poling field on the functional properties of PSN–PT ceramics was made until now. Hence, the aim of our work was also to study the influence of the poling electric field on the electromechanical properties and the phase composition of the 0.57PSN–0.43PT ceramics.

2. Experiment

For the synthesis of the $0.57Pb(Sc_{0.5}Nb_{0.5})O_3$–$0.43PbTiO_3$ (0.57PSN–0.43PT) powder, PbO (99.9%, Aldrich), Sc_2O_3 (99.9% Alfa 11216), TiO_2 (99.8%, Alfa Aesar) and Nb_2O_5 (99.9%, Aldrich) were used. The homogenized, stoichiometric mixture was mechanochemically activated in a high-energy planetary mill (Retsch, Model PM 400) for 24 h at 300 rpm by 15 vidia balls in 250 ml vidia vessel. The powder was then heated in a closed alumina crucible at 900 °C for 1 h. It was analysed by X-ray diffraction with a PANalytical X'Pert PRO MPD using Cu Kα1 radiation. The X-ray spectrum was measured from $2\theta = 10°$ to $2\theta = 70°$ using a step of 0.033° and a dwell of 100 s per step, and it is shown in Fig. 1. The average size of the crystallites was calculated from the average full width at half maximum (FWHM) of the {1 0 0}, {1 1 0} and {2 0 0} diffraction peaks,

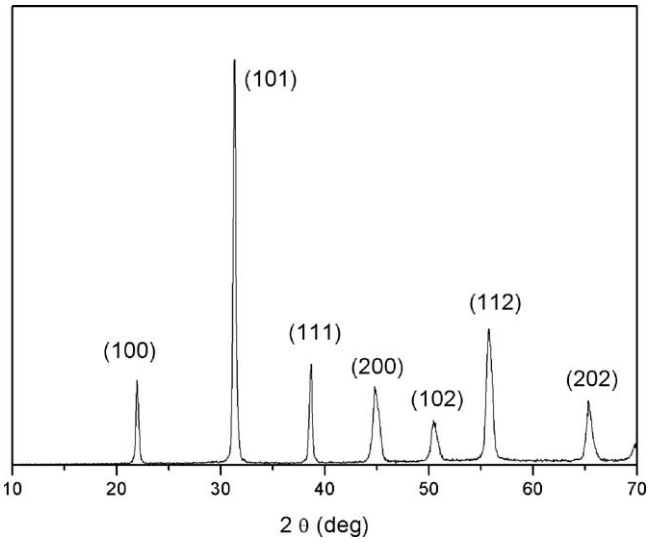

Fig. 1. The X-ray spectra of 0.57PSN–0.43PT powder after mechanochemical activation and thermal treatment.

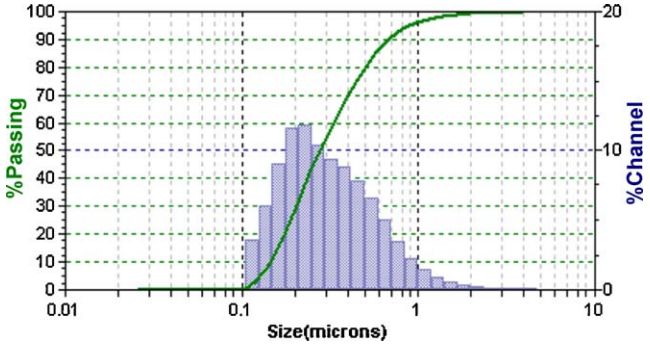

Fig. 2. The particle size distribution of the 0.57PSN–0.43PT powder after thermal treatment and milling.

using the Scherrer's equation.[25] The synthesized powders were milled in an attritor mill with zirconia balls in isopropanol at 800 rpm for 4 h for a de-agglomeration treatment, as reported for PMN–PT in Ref.[26] The particle size distribution determined by laser granulometry (Microtrack S 3500) is shown in Fig. 2.

After the synthesis the crystalline phase and the amorphous phase were present in the powder, as in the case of the PMN–PT material.[20] After the thermal treatment all the amorphous phase, which is produced during the synthesis, is transformed into the crystalline phase, as shown in Fig. 1. The powder is nanocrystalline, with the average size of the crystallites being around 70 nm, calculated by Scherrer's equation. After milling of the powder in an attritor mill the particle size distribution is narrow (Fig. 2) with a median particle size d_{50} equal to 270 nm. The cumulative curve is also included in Fig. 2.

The bulk 0.57PSN–0.43PT ceramics were prepared by pressing isostatically at 300 MPa. The ceramics were then sintered in a double alumina crucible in 0.57PSN–0.43PT packing powder at 1000 °C for 8 h. After sintering the pellets were cut, polished and annealed at 600 °C. The pellets had a diameter of 6 mm and were 0.5 mm thick. The densities of the sintered pellets were determined with Archimedes' method in water at 25 °C.

A JEOL JSM 5800 scanning electron microscope (SEM) equipped with an energy-dispersive X-ray analyser (EDS) was used for the overall microstructural analysis. For the grain-size determination the polished cross-sections of the samples were thermally etched at 900 °C for 20 min and the SEM micrographs were recorded. The median grain size was determined from a digitalized image of the grains using the program UTHSCSA image Tool (UTHSCSA Image Tool Version 3.00, 2002).

For the poling procedure and the electrical measurements, gold electrodes were deposited by sputtering. The diameter of the electrodes was 5 mm. The samples were poled in silicon oil with a DC electric field of 0.5–6 kV/mm at 160 °C for 5 min and then cooled in the same bias field (field cooling, i.e., a FC run). After poling the samples were aged for 24 h.

The ceramics were analysed by X-ray diffraction with a PANalytical X'Pert PRO MPD using Cu Kα1 radiation. The X-ray spectra were measured from $2\theta = 10^\circ$ to $2\theta = 70^\circ$ using a step of 0.033° and a dwell of 100 s per step. The phase composition was determined with a Rietveld analysis of the spectra, using the software Jana2006.[27] We used the starting unit-cell parameters and atomic positions from a previous Rietveld study made by Hamount et al.[3]

The X-ray diffraction measurements of the poled ceramics were performed through the sputtered gold electrode. Due to the presence of the electrodes, which decrease the general quality of the data, the atomic positions proposed by Hamount et al.[3] were not modified. The background, the shift, the unit-cell parameters, the profile parameters, the phase ratio and the preferential orientation were refined to obtain the lowest reliability factors for both phases, i.e., the monoclinic Pm and the tetragonal P4mm.

The dielectric constants were measured with a HP 4284 A Precision LCR Meter at frequencies of 1, 10, and 100 kHz. The coupling coefficients k_p, k_t and mechanical quality factor Q_m were determined with the resonance method,[28] whereas the d_{33} were measured at a frequency of 50 Hz using a Berlincourt piezometer (Take Control PM10, Birmingham, UK). The ferroelectric hysteresis curves were measured with an Aixact TF Analyser 2000 at 1 Hz.

3. Results

3.1. Non-poled 0.57PSN–0.43PT ceramics

The X-ray diffraction pattern of the 0.57PSN–0.43PT ceramics is shown in Fig. 3. First of all, no extra diffraction peaks that might correspond to pyrochlore or PbO phases were detected. For the sake of clarity, the inset in Fig. 3 focuses on the region of the diffraction pattern corresponding to the cubic-like (2 0 0) Bragg peak. It is clear that to properly index the peaks one must consider the coexistence of phases. Rietveld refinements allowed us to show that for these ceramics – a mixture of the tetragonal P4mm phase and the monoclinic Pm phase – it is necessary to describe the whole diffraction pattern. As a result, 71% of the monoclinic Pm and 29% of the tetragonal P4mm phase were determined for the non-poled 0.57PSN–0.43PT ceramics at room temperature, which is in agreement with previously reported results.[4] The reliability factors R_{all}, for the monoclinic

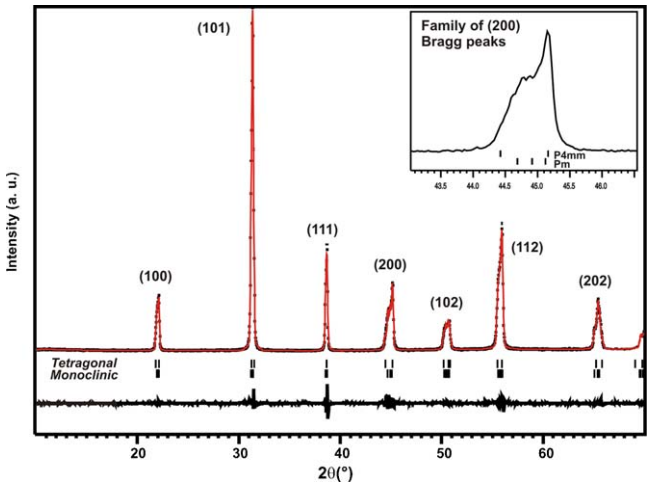

Fig. 3. Observed (dots), calculated (line) and difference curve (bottom) of the X-ray diffraction pattern of the non-poled 0.57PSN–0.43PT ceramics. The tick marks represent the reflections of the tetragonal and monoclinic phases. The indexed peaks of the cubic-like perovskite phase are shown. The inset shows the region of the diffraction pattern corresponding to the cubic-like (2 0 0) Bragg peak.

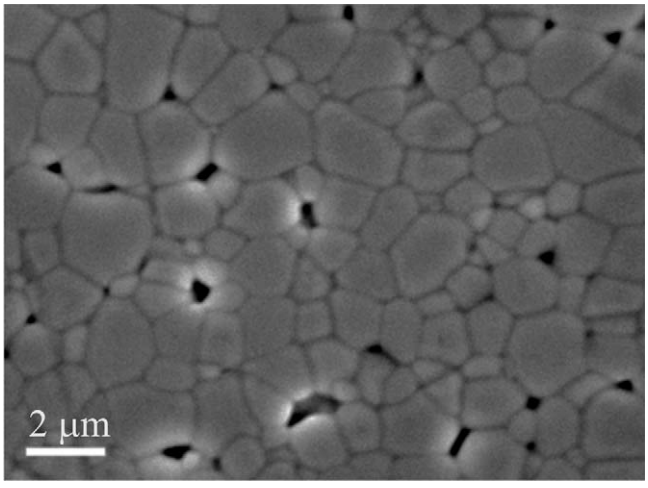

Fig. 4. SEM micrographs of a thermally etched cross-section for the bulk 0.57PSN–0.43PT non-poled ceramics.

Pm (R_M) and tetragonal P4mm (R_T) phases, and the goodness of fit for the profile, GOF, are 1.58, 1.87 and 1.50, respectively. The X-ray diagram reveals no preferential orientation of the unit cells, and attempts to add some orientation only decreased the quality of the refinement.

The measured density of the ceramics was 7.66 g/cm^3, which is 97% of the theoretical density. The theoretical density of 7.94 g/cm^3 was calculated from the cell parameters, obtained from X-ray diffraction, and using the nominal composition. The SEM micrographs of thermally etched cross-sections of the 0.57PSN–0.43PT ceramics are shown in Fig. 4, where it is clear that the ceramics are well sintered. The median grain size is $d_{50} = 1 \pm 0.5$ μm. A dense and chemically homogeneous 0.57PSN–0.43PT ceramic was prepared at 1000 °C, which is 200–300 °C lower than previously reported.[3–10,13,24]

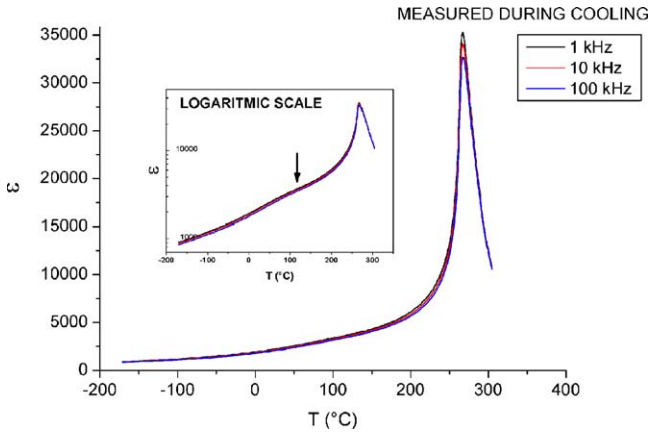

Fig. 5. $\varepsilon(T)$ at 1, 10 and 100 kHz for 0.57PSN–0.43PT ceramics. The inset shows the same graph on a logarithmic scale. The LT phase transition is marked with black arrows.

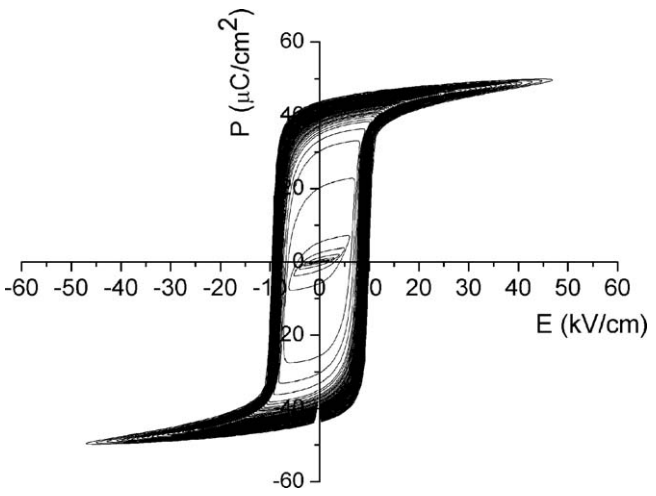

Fig. 6. Hysteresis loop of the 0.57PSN–0.43PT ceramic measured at 1 Hz.

Fig. 5 shows the dielectric constant ε as a function of the temperature T for the 0.57PSN–0.43PT ceramics. The dielectric data were collected during a cooling run. The high-temperature (HT) phase transition from the cubic to the tetragonal phase occurs at 267 °C, which is in agreement with the previously reported values.[3,4,13] The maximum value for the dielectric constant ε_{max} was 35,300. No dependence on the frequency was observed.

The low-temperature (LT) phase transition from the tetragonal P4mm to the monoclinic Pm phases can be observed in the measurements of $\varepsilon(T)$ through a broad anomaly (inset in Fig. 5). The anomaly associated with the LT transition is found at around 120 °C. Harmound et al.[3] reported that, based on X-ray data, below 167 °C the monoclinic Pm phase appears. These data are in agreement with the measurements of $\varepsilon(T)$, as seen in Fig. 5. In related systems, such as PMN–PT,[29–32] the LT phase-transition peak between the monoclinic Pm and the tetragonal P4mm phases was observed before; however, the maximum in the LT broad anomaly was obtained at a lower temperature, i.e., around 50 °C.

The dielectric constant (ε_{room}) and dielectric losses (tg δ_{room}) at room temperature measured at 1 kHz for non-poled 0.57PSN–0.43PT ceramics were 2200 and 0.02, respectively. Only two measurements for ε_{room} and tg δ_{room} and ε_{max} of non-doped PSN–PT ceramics with the MPB composition were reported before.[7,13] The ε_{room} and ε_{max} for the 0.57PSN–0.43PT ceramic prepared by mechano-synthesis were higher than the previous reported data for stoichiometric 0.57PSN–0.43PT ceramics. The data are collected in Table 1.

Fig. 6 shows the hysteresis loop for the 0.57PSN–0.43PT ceramic. The loop is well saturated and the remnant polarization (P_r) and coercive field (E_c) at 1 Hz are 43 μC/cm^2 and 10 kV/cm, respectively. Only two values for P_r and E_c of non-doped PSN–PT ceramics with MPB compositions were reported before.[7,13] The P_r for the 0.57PSN–0.43PT ceramic prepared by mechano-synthesis is higher than the previously reported data for the non-doped and also doped PSN–PT ceramics with MPB compositions. The data are collected in Table 2.

The most important reason for the significantly better low- and high-field dielectric properties of the 0.57PSN–0.43PT ceramics prepared here is the high chemical homogeneity of the material due to the mechanochemical synthesis of the powder. It was shown for PMN–PT material that ceramics as well as thick films prepared by mechanochemical synthesis show excellent properties.[22,26]

3.2. Poled 0.57PSN–0.43PT ceramics

The ceramics were poled at a DC electric field of 0.5–6 kV/mm at 160 °C for 5 min, field cooled (FC), and then aged for 24 h. The X-ray diagram of the family of (1 0 0) and (2 0 0) peaks for the 0.57PSN–0.43PT ceramics poled at an electric field from 0.5 to 6 kV/mm is shown in Fig. 7. It is clear that the X-ray diagram of the ceramics changes with the poling electric field.

As for non-poled ceramics, Rietveld analyses of the X-ray diffraction data show the coexistence of the monoclinic Pm and tetragonal P4mm phases for poled 0.57PSN–0.43PT ceramics. As shown before the non-poled ceramics contain 71% of the monoclinic Pm and 29% of the tetragonal P4mm phase. The amount of monoclinic phase clearly increases after poling at 0.5 kV/mm. These samples contained 85% of the monoclinic Pm and 15% of the tetragonal P4mm phases. At 3 kV/mm there was no large increase in the amount of monoclinic phase, the ceramics contained 86% of the monoclinic Pm and 14% of the tetragonal P4mm phases. The presence of a (0 0 1) orientation of the tetragonal phase is visible in the XRD diagram of the poled samples. This feature was taken into account during the refinement of the monoclinic-to-tetragonal ratio, in order to avoid errors in the calculation of the amounts of the two phases. This improves the quality of the refinements. The X-ray diffraction patterns for the ceramics poled at higher fields look similar to the pattern of the ceramics poled at 3 kV/mm, as seen in Fig. 7.

In Table 3 the calculated phase ratio (monoclinic-to-tetragonal), the reliability factors, R_{all}, for the monoclinic (R_M) and tetragonal (R_T) phases, and the goodness of the fit (GOF) of the profile are reported for the ceramics poled at 0.5 and

Table 1
The dielectric constant at room temperature (ε_{room}), dielectric losses at room temperature (tg δ_{room}) and the maxima of the dielectric constants (ε_{max}) for non-doped and doped PSN–PT ceramics of the MPB compositions obtained by different groups.

Non-doped and doped PSN–PT ceramics	Frequency (kHz)	ε_{room}	tg δ_{room}	ε_{max}
0.57PSN–0.43PT ceram.[this work]	1	2200	0.02	35.300
0.575PSN–0.425PT ceram.[7]	–	2000	0.01	28.000
0.57PSN–0.43PT ceram.[13]	1	1700	0.03	32.700
Nb-doped 0.575PSN–0.425PT ceram.[7]	–	1900	0.02	39.000
Nb-doped 0.575PSN–0.425PT ceram.[9]	1	1700	0.02	17.000
Nb-doped 0.575PSN–0.425PT ceram.[10]	1	2500	0.03	30.500
Fe-doped 0.57PSN–0.43PT ceram.[13]	1	2100	0.01	30.000

–, not given.

Table 2
Ferroelectric properties of non-doped and doped PSN–PT ceramics of the MPB composition obtained by different groups.

Non-doped and doped PSN-PT ceramics	Frequency (Hz)	P_r (μC/cm^2)	E_c (kV/cm)
0.57PSN–0.43PT ceram.[this work]	1	43	10
0.575PSN–0.425PT ceram.[7]	50	19	5
0.57PSN–0.43PT ceram.[13]	1	36	10
Nb-doped 0.57PSN–0.43PT ceram.[8]	50	26	23
Nb-doped 0.575PSN–0.425PT ceram.[10]	–	41	8
Fe-doped 0.57PSN–0.43PT ceram.[13]	1	30	10

–, not given.

Table 3
Phase ratio in percentage, reliability factors, R_{all}, for the monoclinic Pm (R_M) and tetragonal P4mm phases (R_T) and the goodness of the fit (GOF) for the profile of the Rietveld analyses for the X-ray data of the non-poled and poled 0.57PSN–0.43PT ceramics. The calculated uncertainty for the percentage of phases is less than 2%.

Poling	Phase ratio (Pm:P4mm)	R_M	R_T	GOF
Non-poled	71%:29%	1.58	1.87	1.50
0.5 kV/mm	85%:15%	3.30	3.47	0.97
3 kV/mm	86%:14%	3.62	3.72	1.69

3 kV/mm. The data for the non-poled ceramics is added for comparison. The values of the R_M, R_T and the GOF are acceptable, taking into account the fixed atomic positions, the quality of the X-ray measurement and the presence of the additional peaks from the gold electrodes.

The piezoelectric coefficient d_{33} and the coupling coefficients k_p and k_t were measured and are collected in Table 4 as well as shown in Fig. 8. The highest d_{33}, k_p and k_t were measured for the ceramics poled at 3 kV/mm, i.e., 570 pC/N, 0.71 and 0.56, respectively. The ceramics poled at electric fields larger than 3 kV/mm exhibited a lower d_{33} than the ceramics poled at 3 kV/mm. However, the k_p and k_t coefficients stayed constant with an increasing electric field. For the PZT ceramics it was reported that the degradation of the piezoelectric properties with increasing poling field can be related to the micro-cracks induced by the high-field poling procedure.[33–35] The cross-section of the 0.57PSN–0.43PT ceramics poled at 5 kV/mm was investigated with an SEM. However, micro-cracks were not observed.

The d_{33} of the ceramics poled at 3 kV/mm was much higher than the previously reported d_{33} for the stoichiometric 0.57PSN–0.43PT ceramics,[7,13] and it is even comparable with

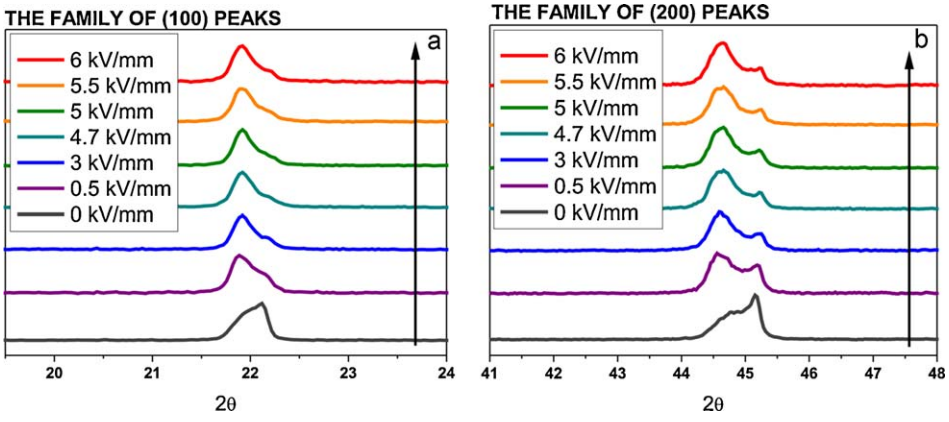

Fig. 7. X-ray diagram of the family of (a) (1 0 0) and (b) (2 0 0) peaks for the poled 0.57PSN–0.43PT ceramics. The X-ray diagram of the non-poled ceramics is added for comparison. The black arrow indicates the increase in the poling electric field from 0 to 6 kV/mm.

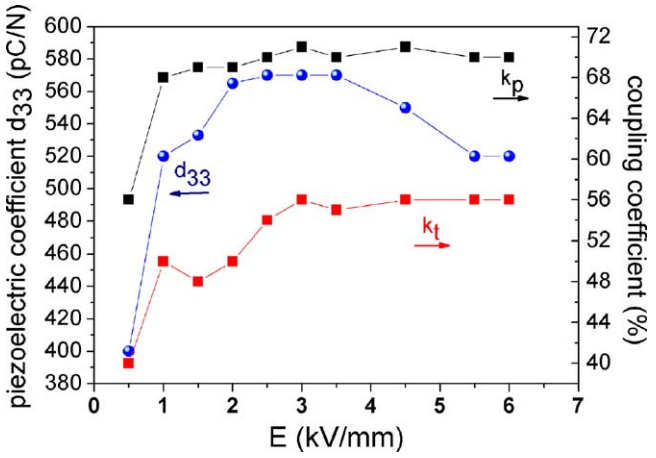

Fig. 8. d_{33}, k_p and k_t as a function of the poling field. The line between the measured values is just a guide to the eye.

Table 4
d_{33}, k_p and k_t for the 0.57PSN–0.43PT ceramics poled at different poling fields.

Poling electric field (kV/mm)	d_{33} (pC/N)	k_p	k_t
0	–	–	–
0.5	400	0.56	0.40
1	520	0.68	0.50
1.5	530	0.69	0.48
2	560	0.69	0.50
2.5	570	0.70	0.54
3	570	0.71	0.56
3.5	570	0.70	0.55
4.5	550	0.71	0.56
5.5	520	0.70	0.56
6	520	0.70	0.56

Table 5
d_{33} of non-doped and doped PSN–PT ceramics of the MPB composition obtained by different groups.

Non-doped and doped PSN–PT ceramics	d_{33} (pC/N)
0.57PSN–0.43PT ceram.[this work]	570
0.575PSN–0.425PT ceram.[7]	390
0.57PSN–0.43PT ceram.[13]	380
Nb-doped 0.57PSN–0.43PT ceram.[8]	590
Nb-doped 0.575PSN–0.425PT ceram.[10]	595
Fe-doped 0.57PSN–0.43PT ceram.[13]	390

the d_{33} of Nb-doped 0.57PSN–0.43PT ceramics,[8,10] as shown in Table 5. The k_p and k_t for the ceramics poled at 3 kV/mm were 0.71 and 0.56, respectively, which are also higher than the previous reported k_p and k_t for stoichiometric 0.57PSN–0.43PT ceramics, i.e., 0.50 and 0.55, respectively.[13] The Q_m of the ceramics poled at 3 kV/mm was 38, which is lower than previously reported data for stoichiometric 0.57PSN–0.43PT ceramics, i.e., around 70[13,36] and higher the data for Nb-doped 0.57PSN–0.43PT ceramics, i.e., 24.[10]

The $\varepsilon(T)$ values measured at 1, 10 and 100 kHz for 0.57PSN–0.43PT ceramics poled at 0.5, 3, 4.7 and 5.5 kV/mm are presented in Fig. 9, where the tetragonal-to-high-temperature-state transition peak is evident. The data were collected during a zero-field heating, in order to keep the same conditions as during the X-ray diffraction measurement. Here, the low-temperature (LT) phase-transition peak between the monoclinic Pm and tetragonal P4mm phases is also evident, as in the case of non-poled ceramics. In Fig. 10 the $\varepsilon(T)$ values during the heating and cooling run of the ceramics poled

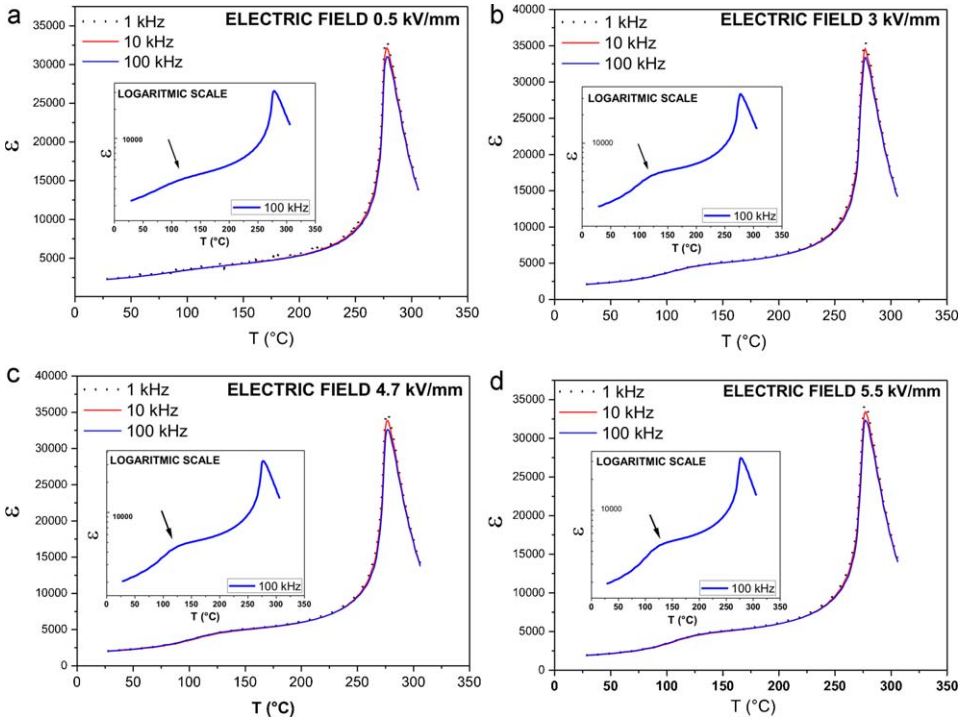

Fig. 9. $\varepsilon(T)$ at 1, 10, and 100 kHz for 0.57PMN–0.43PT ceramics poled at electric fields of (a) 0.5 kV/mm, (b) 3 kV/mm, (c) 4.7 kV/mm and (d) 5.5 kV/mm. The insets show the data measured at 100 kHz on a logarithmic scale.

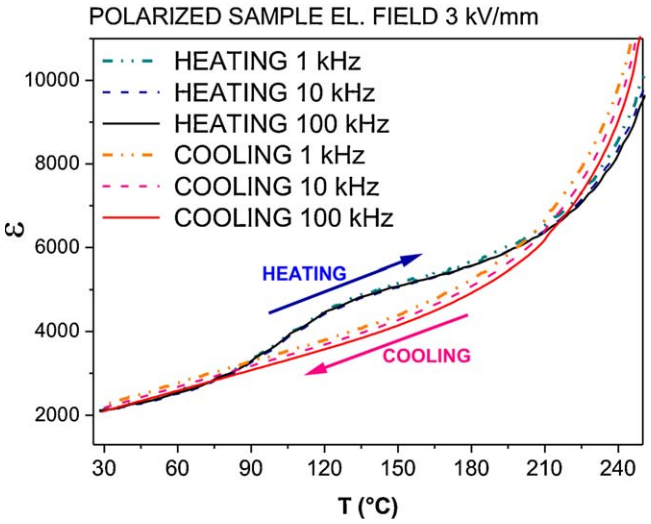

Fig. 10. $\varepsilon(T)$ during heating and cooling run of the ceramics poled at 3 kV/mm at 1, 10 and 100 kHz.

at 3 kV/mm are shown. During the heating run the sample is poled, while during the cooling the sample is depoled and the LT transition peak is less distinctive. In the literature, no such clear evidence (Figs. 9 and 10) for the LT phase transition in the $\varepsilon(T)$ measurement of 0.57PSN–0.43PT ceramics can be found.

4. Conclusion

The synthesis of $0.57Pb(Sc_{0.5}Nb_{0.5})O_3$–$0.43PbTiO_3$ (0.57PSN–0.43PT) ceramics from a mechanochemically activated powder is presented for the first time. At a temperature of 1000 °C we were able to obtain ceramics with 97% of theoretical density and a median grain size of 1 μm. The temperature of 1000 °C is 200–300 °C lower than the previously reported data for the sintering temperature of PSN–PT ceramics. The ceramic at room temperature shows the co-existence of the monoclinic Pm and the tetragonal P4mm phases in the ratio 71% to 29%, respectively, which is in good agreement with previously reported values.

The room-temperature dielectric constant and the maximum value of the dielectric constants are 2200 and 35,300, respectively. These values are higher than the previously reported values for stoichiometric 0.57PSN–0.43PT ceramics. The measurements of the dielectric constant vs. the temperature were carried out for non-poled and poled 0.57PSN–0.43PT ceramics. In the measurements the phase-transition peak between the monoclinic Pm and the tetragonal P4mm phases is evident through a broad anomaly. The peak had a maximum at around 120 °C.

The hysteresis loop of the ceramics was well-saturated, demonstrating the ferroelectric behaviour. The remnant polarization (P_r) and coercive field (E_c) at 1 Hz are 43 μC/cm^2 and 10 kV/cm, respectively. The P_r is higher than the previous reported data for non-doped and also doped PSN–PT ceramics with MPB compositions.

The influence of the poling electric field on the electromechanical properties and on the phase composition of the 0.57PSN–0.43PT ceramics was carefully studied and the correlations between the functional and structural properties are given. The results show that the ratio of the monoclinic to the tetragonal phases can be changed by the application of a poling electric field. The highest piezoelectric coefficient $d_{33} = 570$ pC/N and the coupling coefficients $k_p = 0.71$ and $k_t = 0.56$ of the ceramics are obtained at poling electric fields of 3 kV/mm. The values are much higher than the previously reported d_{33}, k_p and k_t values for stoichiometric 0.57PSN–0.43PT ceramics, and even comparable with the values of doped 0.57PSN–0.43PT ceramics. To conclude, the most important reasons for the significantly better properties of the 0.57PSN–0.43PT ceramics prepared here is the high homogeneity of the material due to the mechanochemical synthesis of the powder.

Acknowledgements

The authors would like thank Ms. Jena Cilenšek and Ms. Alja Kupec for their help with the experimental work. Hana Uršič thanks the Slovenian Research Agency for financial support (postdoctoral project Z2-4125). The financial support of the Slovenian Research Agency in the frame of the program Electronic Ceramics, Nano-, 2D and 3D Structures (P2-0105) is also gratefully acknowledged.

References

1. Park SE, Shrout TR. *Ultrahigh strain and piezoelectric behaviour in relaxor based ferroelectric single crystals*. *J Appl Phys* 1997;**82**:1804–11.
2. Heartling GH. *Ferroelectric ceramics: history and technology*. *J Am Ceram Soc* 1999;**82**:797–818.
3. Haumont R, Dkhil B, Kiat JM, Al-Barakaty A, Dammak H, Bellaiche L. *Cationic-competition-induced monoclinic phase in high piezoelectric $(PbSc_{1/2}Nb_{1/2}O_3)_{1-x}$–$(PbTiO_3)_x$ compounds*. *Phys Rev B* 2003;**68**:0141141–10.
4. Haumont R, Al-Barakaty A, Dkhil B, Kiat JM, Bellaiche L. *Morphotropic phase boundary of heterovalent perovskite solid solutions: experimental and theoretical investigation of $PbSc_{1/2}Nb_{1/2}O_3$–$PbTiO_3$*. *Phys Rev B* 2005;**71**:1041061–12.
5. Bing YH, Ye Z G. *Synthesis and characterizations of the $(1-x)Pb(Sc_{1/2}Nb_{1/2})O_3$–$xPbTiO_3$ solid solution ceramics*. *J Electroceram* 2008;**21**:761–4.
6. Tennery VJ, Hangand KW, Novak RE. *Ferroelectric and structural properties of the $Pb(Sc_{1/2}Nb_{1/2})_{1-x}Ti_xO_3$ system*. *J Am Ceram Soc* 1968;**21**:671–4.
7. Yamashita Y. *Improved ferroelectric properties of niobium-doped $Pb((Sc_{0.5}Nb_{0.5})Ti)O_3$ ceramic material*. *Jpn J Appl Phys* 1993;**32**:5036–40.
8. Yamashita Y. *Piezoelectric properties of niobium-doped $Pb((Sc_{0.5}Nb_{0.5})Ti)O_3$ ceramics material near the morphotropic phase boundary*. *Jpn J Appl Phys* 1994;**33**:4652–6.
9. Adachi M, Miyabukuro E, Kawabata A. *Preparation and properties of $Pb((Sc_{1/2}Nb_{1/2})_{0.575}Ti_{0.425})O_3$ ceramics*. *Jpn J Appl Phys* 1994;**33**:5420–2.
10. Alberta EF, Bhalla AS. *High strain and low mechanical quality factor piezoelectric $Pb((Sc_{1/2}Nb_{1/2})_{0.575}Ti_{0.425})O_3$ ceramics*. *Mater Lett* 1998;**35**:199–201.
11. Jaffe B, Cook WR, Jaffe H. *Piezoelectric ceramics*. Academic Press Inc. (London) Ltd.; 1971.
12. Damjanovic D. *Ferroelecric, dielectric and piezoelectric properties of ferroelectric thin films and ceramics*. *Rep Prog Phys* 1998;**61**:1267.
13. Kim JS, Kim SJ, Kim HG, Lee DC, Uchino K. *Piezoelectric and dielectric properties of Fe_2O_3-doped $0.57Pb(Sc_{1/2}Nb_{1/2})O_3$–$0.43PbTiO_3$ ceramic material*. *Jpn J Appl Phys* 1999;**38**:1433–7.
14. Rajasekaran SV, Jayavel R. *Influence of niobium doping on the electrical properties of $0.58Pb(Sc_{1/2}Nb_{1/2})O_3$–$0.42PbTiO_3$ single crystal*. *Solid State Commun* 2007;**143**:466–70.

15. Leite ER, Scotch AM, Khan A, Chan H, Harmer MP, Liu SF, et al. *Chemical heterogeneity in PMN–35PT ceramics in effects on dielectric and piezoelectric properties*. *J Am Ceram Soc* 2002;**85**:3018–24.
16. Trefalt G, Malič B, Kuščer D, Holc J, Kosec M. *Synthesis of $Pb(Mg_{1/3}Nb_{2/3})O_3$ by self-assembled colloidal aggregates*. *J Am Ceram Soc* 2011, doi:10.1111/j. 1551-2916.2011.04443.x.
17. Xue J, Wan D, Lee SE, Wang J. *Mechanochemical synthesis of lead zirconate titanate from mixed oxides*. *J Am Ceram Soc* 1999;**82**:1687–92.
18. Kuščer D, Meden A, Holc J, Kosec M. *The mechano-synthesis of lead–magnesium–niobate ceramics*. *J Am Ceram Soc* 2006;**89**:3081–8.
19. Xue J, Wang J, Rao TM. *Synthesis of $Pb(Mg_{1/3}Nb_{2/3})O_3$ in excess lead oxide by mechanical activation*. *J Am Ceram Soc* 2001;**84**:660–2.
20. Kuščer D, Holc J, Kosec M. *The formation of 0.65 $Pb(Mg_{1/3}Nb_{2/3})O_3$–$0.35PbTiO_3$ using a high-energy milling process*. *J Am Ceram Soc* 2007;**90**:29–35.
21. Wang J, Wan DM, Xue JM, Ng WB. *Mechanochemical synthesis of $Pb(Mg_{1/3}Nb_{2/3})O_3$–$0.1PbTiO_3$ from mixed oxides*. *Adv Mater* 1999;**11**:210–3.
22. Kosec M, Uršič H, Holc J, Hrovat M, Kuščer D, Malič B. *High-performance PMN–PT thick films*. *IEEE Trans Ultrason Ferroelectr Freq Control* 2010;**57**:2205–12.
23. Alguero M, Ricote J, Castro A. *Mechanosynthesis and thermal stability of piezoelectric perovskite $0.92Pb(Zn_{1/3}Nb_{2/3})O_3$–$0.08PbTiO_3$ powders*. *J Am Ceram Soc* 2004;**87**:772–8.
24. Yamashita Y. *Large electromechanical coupling factor in perovskite binary material system*. *Jpn J Appl Phys* 1994;**33**:5328–31.
25. Guinebretiere R. *X-ray diffraction by polycrystalline materials*. London: ISTE Ltd.; 2007.
26. Alguero M, Moure A, Pardo L, Holc J, Kosec M. *Processing by mechanosynthesis and properties of piezoelectric $Pb(Mg_{1/3}Nb_{2/3})O_3$–$PbTiO_3$ with different compositions*. *Acta Mater* 2006;**54**:501–11.
27. Petricek V, Dusek M, Palatinus LJ. *The crystallographic computing system*. Praha, Czech Republic: Institute of Physics; 2006.
28. *IEEE standard on piezoelectricity IEEE 176–1987*. New York, USA: The Institute of Electrical and Electronics Engineers, Inc.; 1988.
29. Uršič H, Tellier J, Hrovat M, Holc J, Drnovšek S, Bobnar V, et al. *The effect of poling on the properties of $0.65Pb(Mg_{1/3}Nb_{2/3})O_3$–$0.35PbTiO_3$ ceramics*. *Jpn J Appl Phys* 2011;**50**:035801–35806.
30. Xia Z, Wang L, Yan W, Li Q, Zhang Y. *Comparative investigation of structure and dielectric properties of $Pb(Mg_{1/3}Nb_{2/3})O_3$–$PbTiO_3$ (65/35) and 10% $PbZrO_3$-doped $Pb(Mg_{1/3}Nb_{2/3})O_3$–$PbTiO_3$ (65/35) ceramics prepared by a modified precursor method*. *Mater Res Bull* 2007;**42**:1715–22.
31. Alguero M, Alemany C, Pardo L, Thi MP. *Piezoelectric resonances, linear coefficients and losses of morphotropic phase boundary $Pb(Mg_{1/3}Nb_{2/3})O_3$–$PbTiO_3$ ceramics*. *J Am Ceram Soc* 2005;**88**:2780–7.
32. Uršič H, Hrovat M, Holc J, Tellier J, Drnovšek S, Guiblin N, et al. *Influence of the substrate on the phase composition and electrical properties of 0.65PMN–0.35PT thick films*. *J Eur Ceram Soc* 2010;**30**:2081–92.
33. Subbarao EC, Srikanth V, Cao W, Cross LE. *Domain switching and microcracking during poling of lead zirconate titanate ceramics*. *Ferroelectrics* 1993;**145**:271–81.
34. Kroupa F, Nejezchleb K, Saxl I. *Anisotropy of internal stresses in poled PZT ceramics*. *Ferroelectrics* 1998;**88**:123–37.
35. Cao H, Evans AG. *Electric-field-induced fatigue crack growth in piezoelectrics*. *J Am Ceram Soc* 1994;**77**:1783–6.
36. Chen YH, Uchino K, Shen M, Viehland D. *Substituent effects on the mechanical quality factor of $Pb(Mg_{1/3}Nb_{2/3})O_3$–$PbTiO_3$ and $Pb(Sc_{1/2}Nb_{1/2})O_3$–$PbTiO_3$ ceramics*. *J Appl Phys* 2001;**90**(3):1455–8.